Size-dependent effects on the magnetization dynamics of Condon domains

A. Gordon*
Department of Mathematics and Physics, Faculty of Science and Science Education and Center for Computational Mathematics and Scientific Computation, University of Haifa-Oranim, Tivon 36006, Israel

N. Logoboy
Physics and Engineering Research Institute and School of Practical Engineering, Ruppin Academic Center, Emek Hefer, 40250, Israel

W. Joss
Grenoble High Magnetic Field Laboratory, Max Planck Institut für Festkörperforschung and Centre National de la Recherche Scientifique, B.P. 166X, F-38042, Grenoble Cedex 9, France
(Received 16 October 2003; published 19 May 2004)

The existence of magnetic domains in nonferromagnetic metals at quantizing magnetic fields is examined under conditions of de Haas–van Alphen oscillations in the range of strong magnetic fields in thin slabs in a three-dimensional electron gas. Dynamics of Condon domain walls are studied in bulk metals and films at time-varying and time-independent applied magnetic fields. The temperature, magnetic field, purity, and sample size-dependent effects on the width, velocity and mobility of domain walls are calculated. Domain wall resonance and relaxation effects are considered in the three-dimensional electron gas.

DOI: 10.1103/PhysRevB.69.174417 PACS number(s): 75.20.En, 75.60.Ch, 71.10.Ca, 71.70.Di

I. INTRODUCTION

Oscillations of the thermodynamic quantities in an external magnetic field are the result of the oscillations of the density of states and the fact that the magnetic field quantizes the energy levels (Landau quantization).[1] Many properties of the electron gas in normal metals are periodic functions of magnetic fields as successive Landau levels sweep through the Fermi level due to an increase of the external magnetic field—for instance, oscillations of magnetization (de Haas–van Alphen effect—dHvA).[1] The magnetic field changes the density of states and consequently also the internal energy of the electron gas, and when $4\pi\chi>1$ (χ is differential magnetic susceptibility $\partial M/\partial B$, M is the oscillatory part of the magnetization), the ''realignment'' of the density of states, connected with the change of magnetic induction B occurring during the stratification into phases, becomes energetically ''convenient''—the formation of Condon domains.[1,2] This instability caused by magnetic interactions among conduction electrons is known as diamagnetic phase transition.[2] The transformation occurs in each cycle of dHvA oscillations when the reduced amplitude of oscillations approaches unity.[1] A series of phase transitions takes place at discrete values of the external magnetic field. The reason for this collective effect is that an electron is subject to the magnetic induction instead of the magnetic field (the Shoenberg effect).[1] Thus, an applied magnetic field of a few Tesla may ''magnetize'' nonmagnetic metals in the sense of the appearance of magnetic domains. Condon domains were predicted by Condon in Ref. 3 and discovered in silver by means of nuclear magnetic resonance[4] and in beryllium and white tin by means of muon spin-rotation spectroscopy.[5–9] Domain formation at diamagnetic phase transitions was theoretically studied in Refs. 2, 3, 10–20. The diamagnetic phase transition in the single-domain case in three-dimensional (3D) metals was described in Refs. 21–23. The temperature dependence of the magnetic induction bifurcation due Condon domains was satisfactory reproduced in quasi-two-dimensional (2D) (Ref. 24) and 3D metals.[25] It was shown that the temperature dependence of the magnetic induction bifurcation due Condon domains has a universal character and does not depend on the dimensionality of the electron gas. This fact confirms the long-range nature of magnetic interactions between orbital magnetic moments of conduction electrons in metals under high quantizing magnetic fields.[26] It evidences in favor of using the mean-field approach for the description of diamagnetic phase transitions.

Condon domains in the 3D electron gas are the only type of magnetic domains, for which the dynamics of domain walls have not been considered. Note however that oscillations of Condon domain walls were considered in the 2D electron gas by analogy with ferromagnets.[19] The motivation for the investigation of the domain wall dynamics of Condon domains is driven by interest in understanding the characteristic magnetic lengths of the system, deriving from the domain dynamics and their comparison with these parameters calculated from the static properties. The motion of domain walls is determined by the fundamental nature of the magnetic material. Experimental and theoretical investigations of the domain dynamics will give the characteristic sizes of domains and domain walls, hence, the underlying physics of magnetic ordering phenomena under conditions of magnetic oscillations. Consequently, the dynamics of Condon domain walls should be studied as an additional tool for the investigation of the phenomenon.

Ordered states, such as Condon domains, should exhibit several kinds of dynamics: magnetization density waves[10] and motion of domain walls. In weak magnetic fields the wall-displacement processes of ferromagnetic domains[27] govern the magnetization. The Condon domain wall should have a characteristic frequency of oscillations, so far un-

known in 3D metals. Consequently, there should be a resonance dispersion of magnetic susceptibility, caused by wall-displacement processes. Numerous observations have detected the above resonance behavior in ferromagnets and ferroelectrics[28–31] and have furnished experimental evidence of the existence of domain wall mass. Thus, two types of domain dynamics experiments have been done which provide for the most part the basis for the theoretical picture of domain wall motion.[28,31] Small-motion or susceptibility studies mentioned above are the first type, and large-motion or velocity versus applied field are the second. The latter process is motion of domain walls leads to reorientation or switching of the magnetization in domains induced by an applied magnetic field. The above research of Condon domains dynamics deals with bulk metals. The problem of the dynamics of domain walls in thin films remains open and merits investigation as well. It would be useful to examine the dynamics of domain walls in the 3D metals, in which Condon domains have been experimentally detected. The dynamics of the interphase boundaries at first-order diamagnetic phase transitions were theoretically considered in Refs. 12, 16. It would be a mistake to identify the two types of the boundary motion, namely the interphase boundary and domain wall motion. We shall discuss this problem in Sec. III.

The goal of this research of the Condon domain phase and diamagnetic phase transitions is the description of the dynamics of Condon domain walls of the two above-mentioned types. To the best of our knowledge, all the theoretical and experimental studies of diamagnetic phase transitions and Condon domains have been focused on large samples, and all the phenomena have been investigated on a macroscopic scale. Some static mesoscopic properties of metals undergoing diamagnetic phase transitions or containing Condon domains have been studied in Ref. 32.

In this paper we present a mean-field theory elaboration considering the bulk and size-dependent static and dynamic effects in the Condon domain phase. In a more general aspect the Condon magnetism has been recently surveyed in Ref. 33.

The paper is organized as follows. Section I contains an Introduction. Section II deals with the model of Lifschitz-Kosevich-Shoenberg including the Landau-type expansion of the thermodynamic potential density in the bulk and slab cases. Section III concerns the overdamped motion of domain walls. Section IV considers the inertia effect on the motion of domain walls. Section V refers to the finite-size effect on the motion of domain walls. Section VI is devoted to domain wall resonance and relaxation. In Sec. VII we concentrate on phase diagrams and dynamics of domain walls in silver. Section VIII presents conclusions.

II. MODEL

The oscillator part of the thermodynamic potential density can be written neglecting all harmonics in the Lifschitz-Kosevich formula, but one, the first harmonic approximation:[34,1]

$$\Omega = \frac{1}{4\pi k^2}\left[a\cos(b) + \frac{1}{2}a^2\sin^2(b)\right], \tag{1}$$

H is the magnetic field inside the material $b = k(B-H) = k[h_{ex} + 4\pi M]$, ($k = 2\pi F/H^2$, F is the fundamental oscillation frequency, $h_{ex} = H_{ex} - H$ is the small increment of the magnetic field H and the external magnetic field H_{ex}; all the components of vectors are taken along the direction of the magnetic induction). In the first harmonic approximation the magnetization is found from the implicit equation of state:[1]

$$4\pi kM = a\sin[k[h_{ex} + 4\pi(1-n)M]], \tag{2}$$

a is the reduced amplitude of oscillations: $a = 4\pi kA = 4\pi(\partial M/\partial B)_{B=H}$,[1] A is the first harmonic amplitude, n is the demagnetization factor. If the magnetic interaction is strong enough, a state of lower thermodynamic potential can be achieved over part of an oscillation cycle by the sample breaking up into domains, for which the local value of magnetization alternates in sign from one domain to the next. Close to the phase-transition temperature [which is found from the equation $a(T_c, H) = 1$] we can present the thermodynamic potential per unit volume as an expansion in powers of magnetization:

$$\Omega = 2\pi(1-a)M^2 + \tfrac{8}{3}\pi^3 k^2 M^4. \tag{3}$$

Accordingly, we arrived at the Landau-type thermodynamic potential density:[21]

$$\Omega = -\frac{A}{2}M^2 + \frac{B}{4}M^4, \tag{4}$$

$A = 4\pi(a-1); B = \frac{32}{3}\pi^3 k^2$. In the case of the breaking up into domains these equations are valid over the range of domain existence in the dHvA cycle. According to Ref. 34, the temperature and field dependence of the amplitude is

$$a(T,H) = a_0(H)\frac{\lambda T}{\sinh(\lambda T)}\exp[-\lambda(H)T_D], \tag{5}$$

$\lambda \equiv 2\pi^2 k_B m_c c/e\hbar H$, m_c is the cyclotron mass. The limiting amplitude $a_0(H) \equiv a(\lambda T \to 0, H)$ is the combination of temperature-independent factors in the Lifschitz-Kosevich formula,[34] where $a_0 = (H_m/H)^{3/2}$, k_B is the Boltzmann constant, e is the absolute value of the electron charge, c is the light velocity, $\hbar$ is the Planck constant, T_D is the Dingle temperature, and H_m is the limiting field above which diamagnetic phase transition does not occur at any temperature (it depends on the shape of the Fermi surface—see details in Ref. 15). To construct temperature-magnetic-field phase diagrams giving the range of the appearance of diamagnetic phase transitions[15] we use henceforward the implicit equation for the diamagnetic phase-transition temperature (5) putting this equation equal to unity at the phase transition. At $a<1$ ($T>T_d$) the homogeneous phase exists with zero magnetization. At $a>1$ ($T<T_d$) the ''magnetic,'' ordered phase appears with nonzero magnetization. The phase transition of the second order with the well-defined transition temperature T_d takes place only at discrete values of magnetic induction. The envelope of these points serves as the diamagnetic

phase-transition boundary. The left wing of the bell-shaped phase diagram corresponds to comparatively low magnetic fields: $\lambda T_d \gg 1$, the right side corresponds to comparatively high magnetic fields $\lambda T_d \ll 1$. In the first case the phase-transition temperature in a slab T_s is given by[32]

$$T_s = T_d\left[1 - \left(\frac{3^{4/3}}{2^{2/3}\lambda T_d}\right)\left(\frac{r_c}{L}\right)^{2/3}\right], \tag{6}$$

where r_c is the cyclotron radius, L is the slab thickness; here T_d is the bulk phase transition temperature. On the basis of the approach used in Ref. 32 one can derive T_s for high magnetic fields, $\lambda T_d \ll 1$,

$$T_s = T_d\left[1 - \frac{3^{7/3}}{2^{2/3}(\lambda T_d)^2}\left(\frac{r_c}{L}\right)^{2/3}\right]. \tag{7}$$

The question of what the bulk is, should be answered here depending on the value of the second term in the brackets. If its contribution is negligible compared with unity, the phase-transition temperature is size independent, and the properties of the sample are considered as the bulk ones. In the opposite case the slab properties differ from those of the bulk sample. The size dependence of the phase-transition temperature in the slab is the strongest in Eq. (7) since, in contrast to Eq. (6) published in Ref. 32, the second term in the brackets is comparable to unity provided the factors λT_d and r_c/L are small. The cyclotron radius is always much smaller than the slab thickness, and the condition $\lambda T_d \ll 1$ is fulfilled at high magnetic fields corresponding to the right side of the T-H bulk phase diagram. Then suppression of the ordered state is more easily realized in the case of Eq. (7) than in the case of Eq. (6). Using Eq. (7) and putting $T_s = 0$, we get that the sample reaches the minimal value of thickness $L_{\min}$: $L_{\min} = [27(3)^{1/2}/2] r_c/(\lambda T_d)^3$. The size dependence of the A coefficient is therefore related to a diamagnetic phase-transition point shift to lower temperatures at small sizes. The size at which the magnetic ordering becomes unstable is the critical size.

Accordingly, at the critical sizes, a balance among the volume, surface, and gradient energies determines a characteristic phase-transition point ($T_s < T_d$), i.e., a new phase-transition point, instead of the original bulk phase transition point T_d. Beyond this transition temperature the ordered phase will be suppressed in the sample with the dimensions less than the critical sizes. This process is analogous to the classical homogeneous nucleation process in that condensed phase nuclei are not stable unless the radii of the condensed phase nuclei are larger than a specific critical size.

III. DYNAMICS OF DOMAIN WALLS: OVERDAMPED MOTION

Equation (3) is valid in the center of the period of magnetic oscillations: $h = 0$. This means that the sample is in the center of the oscillation cycle so that the up domain and the down domain are equally wide. In the case of the stationary motion of the domain wall acted upon by an ''external force,'' an external magnetic field h removes the equivalence of the states to the right and left of the domain wall. When $h \neq 0$ and it varies, the energy balance is altered and rearrangements of the domain structure take place, mainly through the motion of domain walls. Wall motion is the dominant magnetization mechanism. The wall will move in such a way that the volume of an energetically favorable domain increases at the expense of an energetically unfavorable domain. Thus, we consider the forced motion of the domain wall under the driving force h. Taking into account the declination from the center of the period of oscillations and the energy of domain walls we should add the following two terms to Eq. (4):

$$-hM + \frac{K}{2}\left(\frac{\partial M}{\partial x}\right)^2, \quad K = \frac{r_c^2}{4}.$$

K is the inhomogeneity coefficient. Using the time-dependent Ginzburg-Landau equation $\partial M/\partial t = -\Gamma(\delta\Omega/\partial M)$ for the overdamped motion of domain walls we obtain the following equation:

$$\frac{\partial M}{\partial t} = \Gamma\left(K\frac{\partial^2 M}{\partial x^2} + AM - BM^3 + h\right), \tag{8}$$

Γ is the Landau-Khalatnikov transport coefficient. By using the time-dependent Ginzburg-Landau equation we say that the local rate of displacement of the order parameter is linearly proportional to the local thermodynamic force presented by the functional derivative of the thermodynamic potential density. The constant of proportionality, the kinetic coefficient Γ, is the response coefficient, which defines a time scale for the system. Therefore we suppose that the domain wall dynamics have a relaxational character. This approach was used for the description of motion of interphase boundaries at first-order diamagnetic phase transitions under temperature changes.[12] However we also apply it to the motion of domain walls. One of the reasons for its application was actually shown in Ref. 16. Close to the first-order phase transition the so-called wetting of a domain wall occurs: the domain wall splits into two interphase boundaries between the homogeneous phase and the ''domain-up'' and ''domain-down,'' respectively. The shape of the interphase boundary coincides with that obtained in Ref. 12. By domain-up and domain-down we understand two values of magnetization of opposite directions. This is the wetting of the domain wall by the homogeneous phase. The change from nonwetting to wetting behavior occurs under well-defined conditions corresponding to attaining thermodynamic coexistence of the phase involved. The wetting of an interface by a solid phase may occur when it becomes energetically favorable to insert a thin layer of a new phase at the interface. This condition can often be met when two phases are unstable, as in the vicinity of a critical or a triple point at first-order phase transitions. Comparison of the interphase boundary profile[16] with that obtained in Ref. 12 shows that the interphase boundaries formed by the wetting are kink-solitons of the time-dependent Ginzburg-Landau equation describing the interphase boundary between each of the two domains and the homogeneous phase. Since the interphase boundary and the domain boundary appear in the framework

of this approach we also use it here for the magnetic-field-induced motion of domain walls.

Passing to the moving frame, $s=x-vt$, where v is the velocity in the direction x, we obtain

$$K\Gamma\frac{d^2M}{ds^2}+v\frac{dM}{ds}-\Gamma(-AM+BM^3-ah)=0. \quad (9)$$

The solution to Eq. (9) corresponding to the domain wall boundary conditions is known[35]

$$M(s)=M_2+\frac{M_1-M_2}{1+\exp\left(\frac{s}{\Delta}\right)}. \quad (10)$$

M_1,M_2,M_3 are the roots of the equation $BM^3-AM-ah=0$:

$$M_1=\frac{1}{k\pi}\left(\frac{a-1}{2a}\right)^{1/2}\cos\left(\frac{\varphi}{3}\right),$$

$$M_2=\frac{1}{k\pi}\left(\frac{a-1}{2a}\right)^{1/2}\cos\left(\frac{\pi-\varphi}{3}\right),$$

$$M_3=\frac{1}{k\pi}\left(\frac{a-1}{2a}\right)^{1/2}\cos\left(\frac{\pi+\varphi}{3}\right),$$

$$\varphi=\arccos\left(\frac{h}{h_m}\right),$$

$$h_m=\frac{1}{3k}[2(a-1)]^{3/2}. \quad (11)$$

M_1 and M_2 are magnetization values in two domains corresponding to the two minima of the thermodynamic potential density (4) in an applied magnetic field, while M_3 is the saddle point of the thermodynamic potential density. The solution (10) is a kink-soliton corresponding to a large amplitude disturbance connecting two magnetization states by a domain wall. At h_m the magnetization has only one direction. Thus, the kink solution (10) describes the profile of the domain wall. The width of this moving wall Δ is equal to

$$\Delta=\frac{r_c}{4}\frac{1}{[2\pi(a-1)]^{1/2}}. \quad (12)$$

Its velocity is given by

$$v=(6\pi)^{1/2}\Gamma r_c(a-1)^{1/2}\cos\left(\frac{\pi+\varphi}{3}\right). \quad (13)$$

For $h\ll h_m$

$$v=(6\pi)^{1/2}\Gamma r_c(a-1)^{1/2}\sin\left(\frac{h}{3h_m}\right) \quad (14)$$

or changing the sine in Eq. (14) by the argument and using Eq. (11) we obtain

$$v=\frac{(3\pi)^{1/2}\Gamma r_c kh}{2(a-1)}. \quad (15)$$

Since h is small compared to the applied field inducing magnetic oscillations, we can thus justify the considered shape of the domain wall. The plane wall approximation is valid for small applied fields where a small mount of curvature allows balancing the forces tending to bend the domain wall.

Since the domain walls do not begin to move until the acting field nearly reaches to a threshold magnetic field, below which the domain wall is pinned and above which the wall moves forward, the velocity in Eq. (15) is proportional to the excess magnetic field. This linear dependence is expected in the mean-field theory. The depinning threshold may be treated as a dynamic phase transition and analyzed as a critical phenomenon.

The mobility of Condon domain walls μ can be determined as follows:[36]

$$\mu=\lim_{h\to 0}\left[\frac{v(h)}{h}\right], \quad (16)$$

hence

$$\mu=\frac{(3\pi)^{1/2}\Gamma r_c k}{2(a-1)}. \quad (17)$$

IV. DYNAMICS OF DOMAIN WALLS: INERTIAL EFFECT

Domain wall resonances have not been subjected to any experimental investigations for Condon domains in the 3D electron gas. However, the existence of the domain wall mass can hardly be excluded from general arguments. To describe the rapid, nonoverdamped, movement of the domain wall the inertia term is added. It should include a product of the inertial factor m and the second derivative of the magnetization with respect to time $-\partial^2M/\partial t^2$. Then in the moving frame the first term of Eq. (9) transforms into $K-mv^2$. In this case the domain wall width is given by

$$\Delta=\frac{r_c}{4}\frac{1}{\left\{2\pi(a-1)\left[1+24\pi m\Gamma^2(a-1)\cos^2\left(\frac{\pi+\varphi}{3}\right)\right]\right\}^{1/2}}. \quad (18)$$

The influence of the inertial effect is determined by the dimensionless factor $m\Gamma^2$. Both factors m and Γ are parameters of the theory and should be extracted from the analysis of the system based on experiments. The connection between the inertial factor and the domain wall mass will be found in Sec. VII. Equation (18) becomes Eq. (12) when $m=0$. The velocity of the domain wall is then given by

$$v=\frac{(6\pi)^{1/2}\Gamma r_c(a-1)^{1/2}\cos\left(\frac{\pi+\varphi}{3}\right)}{\left[1+24\pi m\Gamma^2(a-1)\cos^2\left(\frac{\pi+\varphi}{3}\right)\right]^{1/2}}. \quad (19)$$

Equation (19) becomes Eq. (13) when $m=0$. For $h \ll h_m$ Eqs. (18) and (19) give

$$\Delta = \frac{r_c}{4[2\pi(a-1)]^{1/2}} \frac{1}{\left[1+\frac{3\pi\Gamma^2 m k^2 h^2}{(a-1)^2}\right]^{1/2}} \tag{20}$$

and

$$v = \frac{(3\pi)^{1/2}\Gamma r_c k h}{2(a-1)} \frac{1}{\left[1+\frac{3\pi\Gamma^2 m k^2 h^2}{(a-1)^2}\right]^{1/2}}. \tag{21}$$

If $m\Gamma^2 \ll 1$, the inertial effect seems to be negligible. If $m\Gamma^2 \gg 1$, the inertial effect is substantial. k^2h^2 is equal to 0.01–1 for reasonable values of temperature and magnetic field, and its influence on the dynamics of domain walls is smaller than the influence of the factor $m\Gamma^2$. Equation (21) exhibits critical temperature dependence in the overdamped limit. The field dependence of the velocity of domain walls (21) coincides with that derived in Ref. 36 for the fast motion of domain walls in ferromagnets. It is seen from Eq. (20) that the domain wall width narrows when the inertial factor increases.

Comparing Eq. (21) with the equation for the velocity of domain walls measured in ferromagnets,[35]

$$v = \frac{\mu h}{\left[1+\left(\frac{\mu h}{v_m}\right)^2\right]^{1/2}}, \tag{22}$$

where v_m is the limiting velocity of the domain wall, we obtain a very simple formula: $v_m=(K/m)^{1/2}$. Thus, the limiting velocity v_m is determined by the ratio of the inhomogeneity and inertia coefficients. The limiting velocity is the velocity of the domain motion when the second term in the brackets in Eqs. (21) and (22) is much larger than unity. It depends on temperature, magnetic field, and the sample size and will be estimated in Sec. VII. The limiting velocity is derived in the dissipationless case. In the second limiting case of the overdamped domain wall motion, $m=0$, $v=\mu h$. It should be noted that the law field mobility is unaffected by the inertial term. Equations (12), (18), and (20) are presented for $v \ll v_m$, otherwise the domain wall thickness decreases like $[1-(v^2/v_m^2)]^{1/2}$ with increasing the velocity.

V. DYNAMICS OF DOMAIN WALLS AND SIZE-DEPENDENT EFFECTS

The results of Sec. IV are valid for infinite samples. It is clear that sample sizes should be taken into account. The geometry to be considered is that of a slab of infinite planar extent ($L_x, L_y \to \infty$) and of finite thickness L_z. We consider the layerlike domain structure with a phase transition of the second order in the case of a 180° domain. We examine this sample geometry because all the direct measurements of Condon domains[3–9] were made for platelike samples, when two dimensions of the specimen were much larger than its thickness. Using the results of Sec. II, one can obtain equations for the dynamics of domain walls in a slab of finite thickness.

The slab under consideration is a 3D spatial system, being infinite in two dimensions and confined in its thickness. Since the mean-field critical exponents obtained by using the Landau theory are not sensitive to the details of the microscopic system, they are universal.[27] Thus, the critical exponents calculated in the infinite sample are the same in the slab. This means that the size-finite renormalization of the reduced amplitude of magnetic oscillations occurs as a result of the crossover from the bulk to the slab: $a \to \tilde{a}$, where $\tilde{a}$ is the reduced amplitude of dHvA oscillations taking into account the finite-size effect on the slab. Then the width of the domain wall in the case of the overdamped motion is

$$\Delta = \frac{r_c}{4} \frac{1}{[2\pi(\tilde{a}-1)]^{1/2}}. \tag{23}$$

Close to the phase-transition temperature where

$$(\tilde{a}-1) = \left(\frac{\partial a}{\partial T}\right)_{T=T_s} (T_s - T), \tag{24}$$

$$\left(\frac{\partial a}{\partial T}\right)_{T=T_s} = \frac{\lambda^2 T_s}{3}, \quad \lambda T_s \ll 1,$$

$$\left(\frac{\partial a}{\partial T}\right)_{T=T_s} = \lambda, \lambda T_s \gg 1,$$

$$T_s = T_d\left[1-\left(\frac{L_{\min}}{L}\right)^{2/3}\right]. \tag{25}$$

At thick slabs $\tilde{a}=a$, and the bulk properties therefore take place: $T_s=T_d$.

$$v = (6\pi)^{1/2}\Gamma r_c(\tilde{a}-1)^{1/2}\cos\left(\frac{\pi+\varphi}{3}\right). \tag{26}$$

For $h \ll h_m$ the velocity is as follows:

$$v = (6\pi)^{1/2}\Gamma r_c(\tilde{a}-1)^{1/2}\sin\left(\frac{h}{3h_m}\right) \tag{27}$$

or changing $\sin(h/3h_m)$ by $h/3h_m$ we obtain

$$v = \frac{(3\pi)^{1/2}\Gamma r_c k h}{2(\tilde{a}-1)}. \tag{28}$$

Equations (26)–(28) include the dependence of the velocity on the slab thickness L and thus describe the size-dependent dynamics of domain walls in the overdamped motion.

VI. DOMAIN WALL RESONANCE AND RELAXATION

We have considered large motion or velocity versus applied field dynamics of Condon domain walls. The second type of the dynamics of Condon domain walls is a so-called

small-motion case or oscillations of domain walls in the presence of a small time-varying magnetic field. We consider this effect in the 3D case, while oscillations of Condon domain walls in the 2D electron gas were studied in Ref. 19 by analogy with ferromagnets. It is convenient to analyze this subject by proceeding to a simple equation of motion for a 180° wall.[28,29] The small-amplitude periodic motion of unit area of such a domain wall in an applied field is determined, as is that of a simple harmonic oscillator, by its effective mass m_w, its viscous damping coefficient γ, and its stiffness coefficient α. The pressure on the wall is $2M_0H$, M_0 is the magnetization in the domain, where H is the applied field parallel to the direction of the magnetization. We may write therefore,

$$m_w\frac{d^2x}{dt^2}+\gamma\frac{dx}{dt}+\alpha x=2M_0H, \tag{29}$$

as the equation of motion of unit area of a 180° domain wall for small displacements x from equilibrium. The viscous damping parameter γ measures the energy losses connected with the motion of the domain wall. It is difficult to calculate the kinetic coefficient since the damping mechanism is not completely clear. Eddy current damping of domain wall motion in magnetic metals is usually large. However, the motion is also damped by magnetic relaxation mechanisms. Experimental evidence of the existence of domain wall mass was obtained in many materials.[28,29]

The presence of the domain wall mass leads to a domain wall resonance. A characteristic frequency of domain wall oscillations should be observed by measuring magnetic susceptibility caused by wall-displacement processes. Solving Eq. (29) for the case of an alternative magnetic field $H=H_0\exp(i\omega t)$, ω is the frequency, we obtain an expression for the susceptibility χ due to the domain wall displacement[28,29]

$$\chi(\omega)=\frac{\chi_0}{\left(1-\dfrac{\omega^2}{\omega_0^2}+\dfrac{i\omega}{\gamma/m_w}\right)}, \tag{30}$$

where χ_0 is the susceptibility at the frequency $\omega=0$ given by

$$\chi_0=\frac{3(a-1)}{2\pi^2k^2D\alpha}, \tag{31}$$

D is the domain width, and the frequency of the wall resonance[29] (of Condon domains) is given by

$$\omega_0=\left(\frac{\alpha}{m_w}\right)^{1/2}. \tag{32}$$

As is known,[1] $4\pi\chi_0=a$. Then

$$\omega_0=\frac{1}{k}\left[\frac{6(a-1)}{\pi Dam_w}\right]^{1/2}. \tag{33}$$

Taking into account the size-dependent effect we obtain

$$\omega_0=\frac{1}{k}\left[\frac{6(\tilde{a}-1)}{\pi Dam_w}\right]^{1/2}. \tag{34}$$

Let us estimate this frequency under conditions of the experiment[4] in silver: $H=9$ T, $T=1.4$ K, $a=2.6$, $m_w=4.7\times10^{-11}$ g/cm^2 (see below the details of the calculation of m_w) using Eqs. (31) and (32). In this case the resonant frequency is $\omega_0=1.2\times10^7$ s^{-1} corresponding to the real frequency of about 2 MHz. The frequency of the nuclear magnetic resonance in silver, at which the domains were observed, was equal to 18 MHz.[4] The calculated resonant frequency may be therefore observable since the screening due to the skin effect occurs so that the skin layer is much larger than the domain width.

At strong amplitudes of impulse fields the wall motion becomes irreversible and the stiffness becomes independent of the wall position, i.e., the inertial and stiffness terms in Eq. (29) are negligible. Thus, $\gamma v=2M_0h$ in this case; comparing this equation to Eq. (15) we obtain the equation giving the relation between Γ and γ:

$$\Gamma=\frac{2(a-1)^{3/2}}{\pi^{3/2}k^2r_c\gamma}. \tag{35}$$

This limiting case corresponds therefore to the strongly damped case. The motion of the domain wall in metals may be overdamped, since eddy currents weaken inertial effects. The value of m_w/γ may be taken, for example, from magnetic-resonance experiments. It is usually derived from the resonance linewidth.[29] Using Eq. (35) we can present the expression for mobility as follows:

$$\mu=\frac{[3(a-1)]^{1/2}}{\pi k\gamma}. \tag{36}$$

In Ref. 37 the damping coefficient γ is calculated provided eddy currents are the dominant mechanism of damping. In terms of our model this coefficient is given by

$$\gamma=\frac{16AD}{\pi B\rho c^2}, \tag{37}$$

where ρ is the resistivity. For the data of the nuclear magnetic resonance experiment in silver,[4] using $\rho=10^{-12}\ \Omega$ m at helium temperatures for the residual resistivity ratio, equal to about 10 000, characteristic of pure silver samples,[38] we obtain $\gamma=1.2\times10^{-2}$ g/cm^2 s. Inserting the calculated damping into Eq. (36) we have the mobility 150 cm/s G. The mobility is sensitive to the sample purity especially through the resistivity. Using the data of Ref. 4 we get $v\approx15$ m/s. This value shows an order of magnitude of the domain wall velocity in silver by using the given resistivity and the experimental data of Ref. 4. According to Eqs. (36) and (37), the mobility tends to zero on approaching the phase-transition temperature. This behavior is characteristic of the eddy current nature of damping. In the case of the relaxation mechanism of damping the mobility strongly increases when the sample reaches the phase-transition temperature. This follows from Eq. (17). Such a substantial difference between the critical temperature dependence of the

mobility of domain walls in the two cases enables to clarify the role of different mechanisms of damping in the domain wall motion.

In our model the relation between the inertia factor and the domain wall mass is given by

$$m_w = \frac{1}{16\pi^2 k^2} m \frac{(a-1)}{\Delta}. \tag{38}$$

Equation (38) is the result of calculations of the kinetic-energy density

$$\frac{1}{2} m \int \left(\frac{\partial M}{\partial t} \right)^2 dx = \frac{1}{32} m \frac{(a-1)}{\pi^2 k^2 \Delta} v^2, \tag{39}$$

which is equal to $\frac{1}{2} m_w v^2$. The calculation of Eqs. (38) and (39) is based on the calculation of the difference between the energy of the moving domain wall and the energy of the domain wall at rest, which is equal to $\frac{1}{2} m_w v^2$.

The limiting velocity of Condon domain walls v_m under conditions of the experiment[4] in silver can be estimated by using $v_m = (K/m)^{1/2}$ (see Sec. IV): $v_m = 100$ m/s. In the calculations of the resonant frequency and the domain wall mass m_w is taken as 4.7×10^{-11} g/cm^2. This value is calculated following the known consideration of the domain wall inertia in conducting media[39] on the basis of the data of the nuclear magnetic-resonance experiment.[4] In our case the calculation made according to Ref. 39 gives the following result:

$$m_w = \frac{\pi D^3 A}{3 B \rho^2 c^4}. \tag{40}$$

The relaxation time $\tau = \gamma/\alpha$ is the time, with which the domain wall responds to changes of the external ''force'' $2M_0 h$. If the domain wall response to the applied field is rapid, the inertial effects are negligible. At frequencies low enough compared to the domain wall resonant frequency the motion of the domain wall behaves as a simple relaxation with the real and imaginary parts of the susceptibility

$$\chi'(\omega) = \chi_0 \frac{1}{1 + (\omega\tau)^2}, \tag{41}$$

$$\chi''(\omega) = \chi_0 \frac{\omega\tau}{1 + (\omega\tau)^2}. \tag{42}$$

The calculation of $\omega_0 \tau$ gives $4\sqrt{3a}/\pi^2$. This expression is distinct from that derived in Ref. 19 for the 2D electron gas, $\sqrt{3/4\pi}$, and includes the reduced amplitude of dHvA oscillations, a depending on temperature, magnetic field, and size sample for a thin specimen. For the data[4] $\omega_0 \tau \propto 1$. The response type is therefore unclear. However, increasing the reduced amplitude may lead to $\omega_0 \tau \gg 1$ and provide the resonance response. In the opposite case $\omega_0 \tau \ll 1$, which also may be reached by changing temperature and magnetic field, the eddy currents pattern appear to move along as though it was attached to the moving domain wall. Thus, the inertial effect is negligible, and the domain wall motion is overdamped. For this reason, the consideration in Sec. III is valid. In a sense, the relaxational character of the domain wall response is supported by the analysis of the helicon resonance in aluminum under conditions of the Condon domains' appearance.[40] The softening of the helicon has been shown in Ref. 40 to happen owing to the occurrence of Condon domains. The growth of the helicon damping has been found related to the relaxational dynamics of diamagnetic phase transitions.[40] It cannot be explained by the eddy currents induced by helicons. The characteristic helicon frequencies in Ref. 41 are several hundreds of Hertz. From the data presented in Ref. 42, the frequency that makes oscillations of domain walls possible is about 1 MHz. It is much larger than the helicon frequency. This means that domain wall motion will not occur at least at frequencies smaller than 1 MHz. This conclusion is clear from the conditions of the experiment, in which the wavelengths of the helicons are much larger than the domain width. Consequently, the damping of helicons observed in Ref. 41 is not caused by eddy currents induced by motion of the domain walls in the oscillating field of helicons. The similar calculation of the frequency of oscillations of domain walls was made in Ref. 42 in beryllium. The authors[42] showed that in beryllium domain wall motion will not occur until 20 MHz. Similar result was actually observed in Ref. 4 in silver, where the Larmor frequency, 18 MHz, did not cause domain motion. The analysis of the helicon damping in aluminum showed a strong temperature increase exhibiting critical slowing down in the electron relaxation time.[40] This characterizes the overdamped dynamics of magnetically interacting electrons in aluminum. The response of the domain walls apparently reflects the response of the collectivized electrons determining the Shoenberg effect. It should evidently be of a relaxational type in aluminum. However, this fact does not necessarily lead to conclusions about the relaxational dynamics of domain walls in other metals in which Condon domains occur. A generalized conclusion on the type of dynamics of domain walls is not evident. The type of dynamics of domain walls remains an open problem requiring further clarification.

VII. MAGNETIZATION REORIENTATION IN SILVER

To construct the T-H phase diagram in silver we put $a = 1$ in Eq. (5) and plot the dependence of T on H.[25]

The curves in Fig. 1 form the geometric place of points of diamagnetic phase transitions for different Dingle temperatures (from 0 K to 1 K) reflecting the degree of purity of the sample in silver: outside the bell-shape curve the homogeneous phase takes place, while the ordered phase is located inside the bell. The interphase curves separate the two phases. The phase diagram is constructed on the basis of Eq. (5) equal to unity. The range of existence of the ordered phase decreases with increasing the Dingle temperature. As we stated in Sec. II, the region of high magnetic fields in the phase diagram exhibits a more pronounced size-dependent effect. In this range of fields the bulk phase-transition temperature is given by[22]

$$T_d = \frac{[6[a_0 \exp(-\lambda T_D) - 1]]^{1/2}}{\lambda}. \tag{43}$$

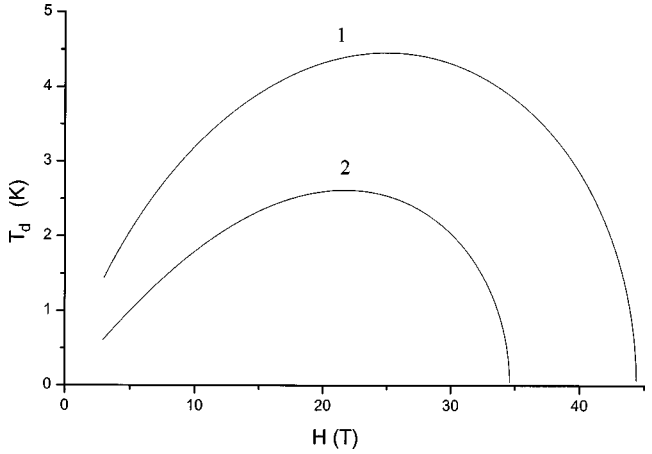

FIG. 1. The temperature-magnetic-field phase diagram in silver for different Dingle temperatures. The bulk phase transition T_d is given in K, the magnetic field is given in Tesla, T. The curve 1 denotes $T_D=0$ K, $2-1$ K.

In this case the largest shift of the phase-transition temperature should take place.

In Fig. 2 the phase-transition temperature in the slab $T_s(H)$ is shown as a function of the magnetic-field value at zero Dingle temperature at two ranges of comparatively low fields and comparatively high fields at different values of the slab thickness from 1 μm to 10 μm in silver. For constructing the plot equations (5), (6), and (7) are used. It is seen that the phase-transition temperature decreases with increasing the magnetic-field value. The growth in the Dingle temperature leads to decreasing the phase-transition temperature. The analytic results are obtained in these two cases. In this figure the results are ''sewn'' and are seen to form the common phase diagram also giving information about the range of $\lambda T_d \propto 1$.

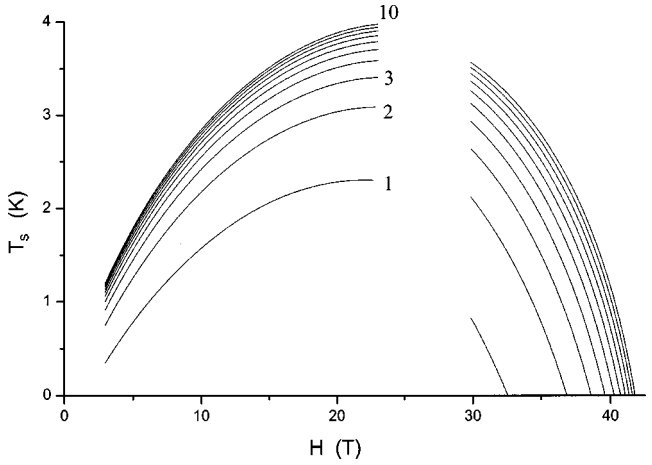

FIG. 2. The phase-transition temperature in the slab $T_s(H)$ as a function of the magnetic-field value at zero Dingle temperature at two ranges: the left wing describes the region of comparatively low fields in the bulk phase diagram, $\lambda T_d \gg 1$, T_d is the bulk phase-transition temperature, the right wing describes the region of comparatively high fields in the bulk phase diagram, $\lambda T_d \ll 1$, at different values of the slab thickness from 1 μm to 10 μm in silver (ten curves). The analytic results are obtained for the two cases. The data in the two ranges are ''sewn'' and are seen to form the common phase diagram also giving information about the range of $\lambda T_d \propto 1$.

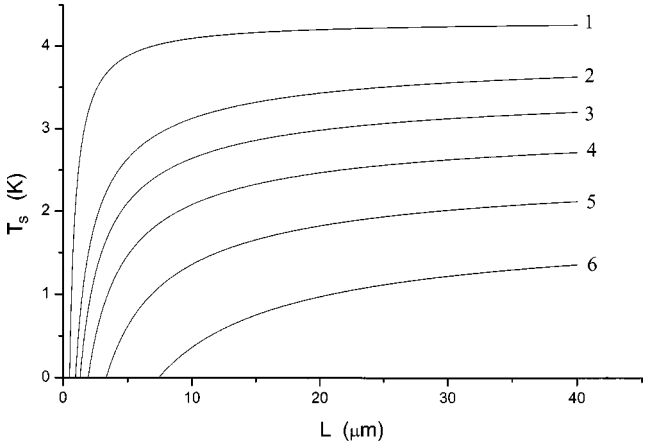

FIG. 3. The phase-transition temperature in the slab is presented as a function of the slab thickness $T_s(L)$. The phase-transition temperature is given in K units at six different Dingle temperatures from 0 K to 1 K in the region of high magnetic fields in silver: $1-0$ K, $2-0.2$ K, $3-0.4$ K, $4-0.6$ K, $5-0.8$ K, $6-1$ K. The thickness L is given in micrometer.

In Fig. 3 the phase-transition temperature in the slab is presented as a function of the slab thickness $T_s(L)$ for different Dingle temperatures from 0 K to 1 K in the region of high magnetic fields in silver. Equations (6) and (7) are used for the plot construction. The graph is the phase diagram for the confined sample. Under the curves the range of the ordered phase is located for each Dingle temperature. The homogeneous phase is situated above and to the left of the curves. It is seen that the phase-transition temperature in the slab decreases with decreases of the slab thickness reaching zero at a definite thickness. This minimum thickness $L_{\min}$ depends on the magnetic field and the Dingle temperature. The graph is plotted for high magnetic fields of the bulk

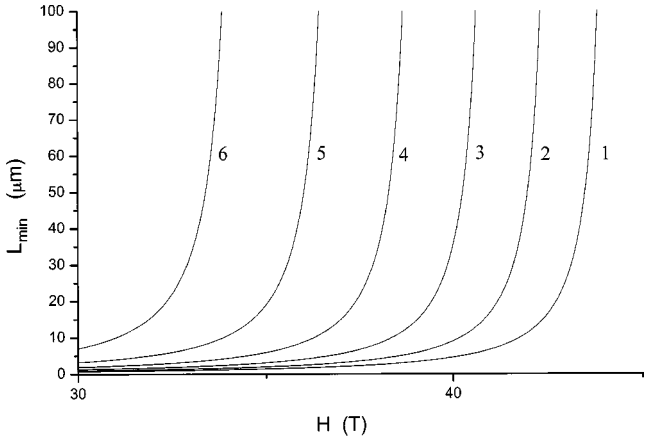

FIG. 4. The magnetic-field dependence of the minimal slab thickness $L_{\min}$ given in micrometer is presented in the case of strong fields and at different Dingle temperatures from 0 K to 1 K in silver: $1-0$ K, $2-0.2$ K, $3-0.4$ K, $4-0.6$ K, $5-0.8$ K, $6-1$ K. The magnetic-field value is given in Tesla, T.

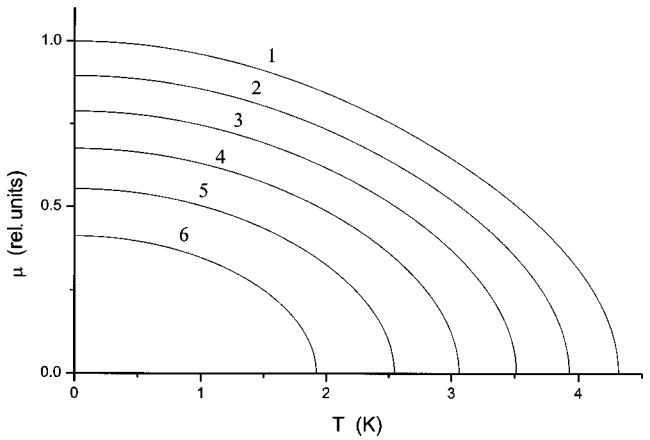

FIG. 5. The mobility of domain walls μ is shown as a function of temperature at the magnetic field 30 T and different Dingle temperatures from 0 K to 1 K in silver: $1-0$ K, $2-0.2$ K, $3-0.4$ K, $4-0.6$ K, $5-0.8$ K, $6-1$ K. Mobility is given in units of $3^{1/2}/\pi k\gamma$.

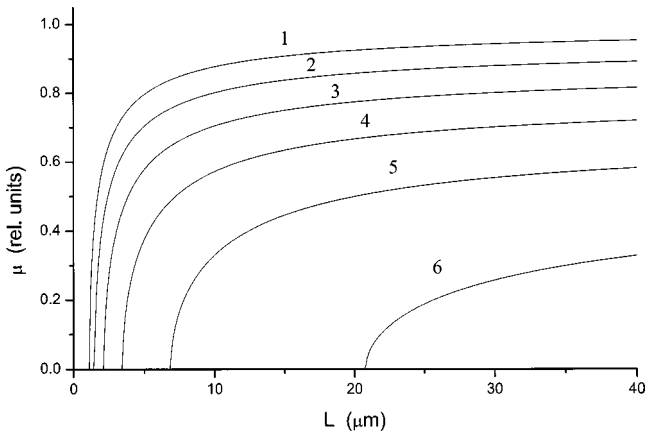

FIG. 6. The mobility of domain walls μ is presented as a function of the slab thickness L at different Dingle temperatures and at magnetic field 30 T and temperature 1 K in silver: $1-0$ K, $2-0.2$ K, $3-0.4$ K, $4-0.6$ K, $5-0.8$ K, $6-1$ K. The mobility is given in units of $3^{1/2}/\pi k\gamma$.

phase diagram. Depending on the Dingle temperature the phase-transition temperature in the slab reaches the bulk phase-transition temperature starting from the slab thickness approximately equal to 100 μm. Above this limit value the sample properties are the bulk ones. Below this thickness the crossover occurs from the bulk size-independent properties to the finite-size ones.

In Fig. 4 the magnetic-field dependence of the minimal slab thickness $L_{\min}$ is presented in the case of strong fields and at different Dingle temperatures from 0 K to 1 K in silver. It increases with increases in the magnetic-field value. We use Eqs. (5), (6), and (7) for the graph construction.

In Fig. 5 the mobility of domain walls μ is shown as a function of temperature at the magnetic field 30 T and different Dingle temperatures from 0 K to 1 K in silver. Mobility is given in units of $3^{1/2}/\pi k\gamma$. Equations (36), (24), and (25) are used for the calculation. The mobility increases as the temperature is lowered. It tends to zero at the phase-transition temperature exhibiting the critical temperature dependence. The effect of critical slowing down takes place in the domain wall mobility.

In Fig. 6 the mobility μ is presented as a function of the slab thickness at different Dingle temperatures at the magnetic field 30 T and temperature 1 K in silver. It is given in units of $3^{1/2}/\pi k\gamma$. Equations (36), (24), and (25) are used for the calculation. Mobility decreases with decrease in the slab thickness tending to zero at the minimal thickness.

In Fig. 7 the h dependence of the velocity of domain walls $v(h)$ is presented in units of the mobility μ in silver at the magnetic-field value 9 T and temperature 1 K at two Dingle temperatures: 0 K$-$1, 0.2 K$-$2. The velocity is given in units of h/h_m. Equations (22) and (17) are used for the calculation. Increasing the inertial effect would lead to change in the curvature of the graph indicating a tendency towards saturation in strong fields upon field increase. The curve shown in this figure is plotted at a field for which the damping is strong enough to avoid saturation of the velocity with field increase, characteristic of inertia-response type systems. The curves end when the reorientation is complete and the magnetization has only one direction. It is seen that the deterioration of sample purity reflected in growth of the Dingle temperature reduces the range of the domain existence cutting the region of the allowed fields at which the two-domain region takes place.

Since the temperature dependence of the resonant frequency coincides with that of mobility, the temperature and size curves of the frequency in relative units are similar to those presented in Figs. 5 and 6.

VIII. CONCLUSIONS

The finite-size effect on the diamagnetic phase-transition temperature is considered in high quantizing magnetic fields in a slab. Critical slab thickness is found below which the magnetic ordering disappears. The shift of the phase-

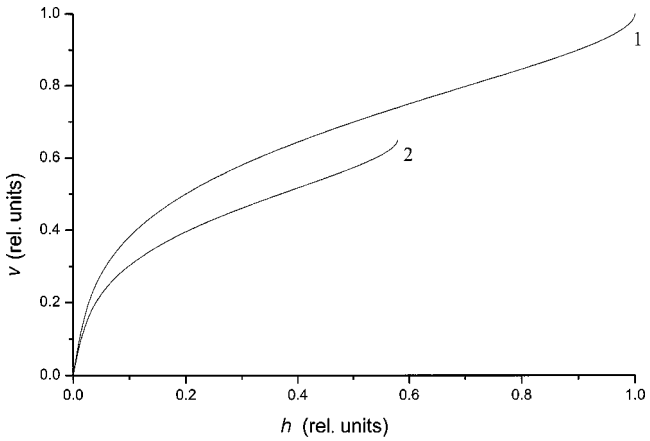

FIG. 7. The velocity of domain walls v in units of v_m, as a function of the decrement of the magnetic field h, which is the deviation from the period center of oscillations at magnetic field 9 T and temperature 1.2 K in silver at zero Dingle temperature. The field h is given in Gauss, G. v_m is the limiting velocity of domain walls.

transition temperature towards lower temperatures is shown to be especially sensitive to the sample thickness in high magnetic fields corresponding to the right wing of the *T*-*H* phase diagram.

Dynamics of domain walls of two types are studied. Large-motion or velocity versus applied field is the first type. Small-motion of domain walls exhibited in the dynamic susceptibility is the second type. The overdamped motion of domain walls is considered in the bulk and film cases. The inertia effect on the wall motion is also examined in the two cases. The mobility of domain walls is derived and estimated. The characteristic frequency of domain wall oscillations under the alternative magnetic-field application is calculated.

ACKNOWLEDGMENTS

The authors are grateful to the Forschungszentrum Jülich, K. Urban, and B. Grushko for their hospitality and to P. Wyder for his interest in this work. Helpful conversations with I. Sheikin and R. Kramer are acknowledged. One of us (A.G.) is indebted to A. Stepanov for stimulating discussions.

*Corresponding author. FAX number: + 972-4-9832167. Email address: algor@math.haifa.ac.il

[1] D. Shoenberg, *Magnetic Oscillations in Metals* (Cambridge University Press, Cambridge, England, 1984).
[2] A. Privorotskii, *Thermodynamic Theory of Domain Structures* (Wiley, New York Israel University Press, Jerusalem, 1976).
[3] J. H. Condon, Phys. Rev. **45**, 526 (1966).
[4] J. H. Condon and R. E. Walstedt, Phys. Rev. Lett. **21**, 612 (1968).
[5] G. Solt, C. Baines, V. S. Egorov, D. Herlach, E. Krasnoperov, and U. Zimmermann, Phys. Rev. Lett. **76**, 2575 (1996).
[6] G. Solt, C. Baines, V. S. Egorov, D. Herlach, E. Krasnoperov, and U. Zimmermann, Hyperfine Interact. **104**, 257 (1997).
[7] G. Solt, C. Baines, V. S. Egorov, D. Herlach, E. Krasnoperov, and U. Zimmermann, Phys. Rev. B **59**, 6834 (1999).
[8] G. Solt, V. S. Egorov, C. Baines, D. Herlach, and U. Zimmermann, Phys. Rev. B **62**, R11 933 (2000).
[9] G. Solt, C. Baines, V. S. Egorov, D. Herlach, and U. Zimmermann, J. Appl. Phys. **87**, 7144 (2000).
[10] S. C. Ying and J. J. Quinn, Phys. Rev. Lett. **22**, 231 (1969).
[11] A. Gordon and I. D. Vagner, J. Phys.: Condens. Matter **2**, 3787 (1990).
[12] A. Gordon, I. D. Vagner, and P. Wyder, Phys. Rev. B **41**, 658 (1990).
[13] A. Gordon, I. D. Vagner, and P. Wyder, Solid State Commun. **74**, 401 (1990).
[14] A. Gordon, B. Grushko, I. D. Vagner, and P. Wyder, Phys. Lett. A **160**, 315 (1991).
[15] B. Grushko, A. Gordon, I. D. Vagner, and P. Wyder, Phys. Rev. B **45**, 3119 (1992).
[16] A. Gordon, T. Salditt, I. D. Vagner, and P. Wyder, Phys. Rev. B **43**, 3775 (1991).
[17] M. A. Itskovsky, G. F. Kventsel, and T. Maniv, Phys. Rev. B **50**, 6779 (1994).
[18] I. D. Vagner, T. Maniv, and E. Ehrenfreund, Phys. Rev. Lett. **51**, 1700 (1983).
[19] R. S. Markiewicz, Phys. Rev. B **34**, 4172 (1986).
[20] T. Maniv and I. D. Vagner, Phys. Rev. B **41**, 2661 (1990).
[21] A. Gordon, M. A. Itskovsky, and P. Wyder, Phys. Rev. B **55**, 812 (1997).
[22] A. Gordon, M. A. Itskovsky, and P. Wyder, Solid State Commun. **103**, 167 (1997).
[23] A. Gordon, M. A. Itskovsky, and P. Wyder, J. Phys. Soc. Jpn. **66**, 136 (1997).
[24] A. Gordon, M. A. Itskovsky, I. D. Vagner, and P. Wyder, Phys. Rev. Lett. **81**, 2787 (1998).
[25] A. Gordon, M. A. Itskovsky, and P. Wyder, Phys. Rev. B **59**, 10 864 (1999).
[26] S. C. Ying, B. J. McIntyre, and J. J. Quinn, Phys. Rev. B **2**, 1801 (1970).
[27] L. D. Landau and E. M. Lifshitz, Phys. Z. Sowjetunion **8**, 153 (1935).
[28] A. P. Malozemoff and J. C. Slonczewski, *Magnetic Domain Walls in Bubble Materials* (Academic Press, New York, 1979).
[29] S. V. Vonsovskii, *Magnetism* (Wiley, New York, 1974).
[30] M. E. Lines and A. M. Glass, *Principles and Application of Ferroelectrics and Related Materials* (Clarendon, Oxford, 1977).
[31] B. Barbara, D. Gignoux, and C. Vettier, *Lectures on Modern Magnetism* (Science Press, Beijing/Springer-Verlag, Berlin 1988).
[32] A. Gordon and P. Wyder, Phys. Rev. B **64**, 224427 (2001).
[33] A. Gordon, I. D. Vagner, and P. Wyder, Adv. Phys. **52**, 385 (2003).
[34] I. M. Lifshitz and A. M. Kosevich, Zh. Eksp. Teor. Fiz. **29**, 730 (1955) [Sov. Phys. JETP **2**, 236 (1956)].
[35] M. A. Collins, A. Blumen, J. F. Currie, and J. Ross, Phys. Rev. B **19**, 3630 (1979).
[36] V. G. Bar'yakhtar, B. A. Ivanov, and M. V. Chetkin, Usp. Fiz. Nauk **146**, 417 (1985) [Sov. Phys. Usp. **28**, 563 (1985)].
[37] H. J. Williams, W. Shockley, and C. Kittel, Phys. Rev. **80**, 1090 (1950).
[38] B. R. Barnard, A. D. Caplin, and M. N. B. Dalimin, J. Phys. F: Met. Phys. **12**, 719 (1982).
[39] W. J. Carr, Jr., in *Magnetism and Magnetic Materials-1976*, edited by J. J. Becker and G. H. Lander, AIP Conf. Proc. No. 34 (AIP, New York, 1976), p. 108.
[40] A. Gordon, W. Joss, N. Logoboy, and I. D. Vagner, Physica B **337**, 303 (2003).
[41] V. I. Bozhko and E. P. Volskii, Zh. Eksp. Teor. Fiz. **26**, 337 (1977) [Sov. Phys. JETP **26**, 335 (1977)].
[42] L. R. Testardi and J. H. Condon, Phys. Rev. **B1**, 3928 (1969).